AD-A150 878 DAMAGE ESTIMATION IN CARBON FIBRE REINFORCED EPOXY AND ITS INFLUENCE ON R..(U) ECOLE NATIONALE SUPERIEURE DES MINES EVRY (FRANCE) CENTRE DES.. A R BUNSELL ET AL. 1/1

UNCLASSIFIED AUG 83 AFOSR-TR-85-0135 AFOSR-82-0141 F/G 11/4 NL

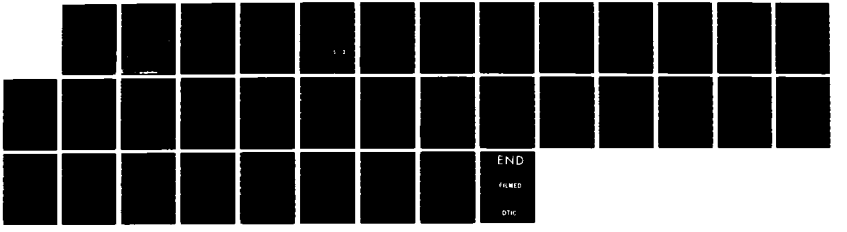

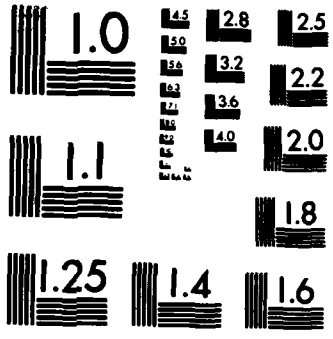

MICROCOPY RESOLUTION TEST CHART
NATIONAL BUREAU OF STANDARDS-1963-A

Centre des Matériaux de l'Ecole des Mines de Paris
B.P. 87 - 91003 EVRY CEDEX

Contract A.F.O.S.R./A.R.M.I.N.E.S.
N° A.F.O.S.R.-82-0141
Final Report
August 1983

DAMAGE ESTIMATION IN CARBON FIBRE REINFORCED EPOXY AND ITS INFLUENCE ON RESIDUAL PROPERTIES

UNCLASSIFIED
SECURITY CLASSIFICATION OF THIS PAGE

REPORT DOCUMENTATION PAGE

1a. REPORT SECURITY CLASSIFICATION UNCLASSIFIED	1b. RESTRICTIVE MARKINGS
2a. SECURITY CLASSIFICATION AUTHORITY	3. DISTRIBUTION/AVAILABILITY OF REPORT Approved for Public Release; Distribution Unlimited.
2b. DECLASSIFICATION/DOWNGRADING SCHEDULE	
4. PERFORMING ORGANIZATION REPORT NUMBER(S)	5. MONITORING ORGANIZATION REPORT NUMBER(S) AFOSR-TR- 85-0135
6a. NAME OF PERFORMING ORGANIZATION ECOLE NATIONAL DES MINES DE PARIS 6b. OFFICE SYMBOL (If applicable)	7a. NAME OF MONITORING ORGANIZATION AFOSR/NA
6c. ADDRESS (City, State and ZIP Code) 60 BOULEVARD ST. MICHEL 75006 PARIS CEDEX 06 FRANCE	7b. ADDRESS (City, State and ZIP Code) Bolling AFB, DC 20332
8a. NAME OF FUNDING/SPONSORING ORGANIZATION AIR FORCE OFFICE OF SCIENTIFIC RESEARCH 8b. OFFICE SYMBOL (If applicable) NA	9. PROCUREMENT INSTRUMENT IDENTIFICATION NUMBER AFOSR 82-0141
8c. ADDRESS (City, State and ZIP Code) BOLLING AFB DC 20332-6448	10. SOURCE OF FUNDING NOS. PROGRAM ELEMENT NO. 61102F; PROJECT NO. 2307; TASK NO. B2; WORK UNIT NO.
11. TITLE (Include Security Classification) DAMAGE ESTIMATION IN CARBON FIBRE REINFORCED EPOXY AND ITS INFLUENCE ON RESIDUAL PROPERTIES	
12. PERSONAL AUTHOR(S) A R BUNSELL; D VALENTIN	
13a. TYPE OF REPORT FINAL	13b. TIME COVERED FROM 15JUN82 TO 14JUN83
14. DATE OF REPORT (Yr., Mo., Day) 1983, AUGUST	15. PAGE COUNT 26
16. SUPPLEMENTARY NOTATION Cont'd	
17. COSATI CODES FIELD / GROUP / SUB. GR.	18. SUBJECT TERMS (Continue on reverse if necessary and identify by block number) ACOUSTIC EMISSION, CONTINUOUS FIBER COMPOSITES, COMPOSITES, FIBER FRACTURE, COMPOSITES FAILURE, RESIDUAL STRENGTH.
19. ABSTRACT (Continue on reverse if necessary and identify by block number) (SEE REVERSE)	
20. DISTRIBUTION/AVAILABILITY OF ABSTRACT UNCLASSIFIED/UNLIMITED XX SAME AS RPT. ☐ DTIC USERS ☐	21. ABSTRACT SECURITY CLASSIFICATION UNCLASSIFIED
22a. NAME OF RESPONSIBLE INDIVIDUAL DAVID A GLASGOW, MAJOR, USAF	22b. TELEPHONE NUMBER (Include Area Code) (202) 767-4937 22c. OFFICE SYMBOL AFOSR/NA

DD FORM 1473, 83 APR EDITION OF 1 JAN 73 IS OBSOLETE.

UNCLASSIFIED
SECURITY CLASSIFICATION OF THIS PAGE

Tensile and creep tests of unidirectional and cross plied specimens were conducted and all tests were monitored for acoustic emission. Failure of unidirectional composites is related directly to failure of fibers which can be regularly and reproducibly correlated with acoustic emission count. A relationship had been postulated earlier relating emission rate and total emission count. A parameter n has been added to this relationship which still allows remarkable correlation even for some nonunidirectional laminates. As the angles of fiber layup increase and mechanisms other than fiber breakage become more important the value of n decreases from unity. For unidirectional laminates a model for total number of fiber breaks can be related to a critical load transfer length using certain probabilities of fiber breakage given no adjacent fiber breaks, one adjacent fiber break, two adjacent fiber breaks, and so on. The resulting predictions correlate very well with a Weibull distribution description of the actual data with a Weibull shape parameter of four. From the model this would indicate that three adjacent breaks lead to final failure, which is considered highly likely. The effects of time and temperature on load transfer length are very important since the gradual increase in load transfer length has the effect of increasing the stresses in unbroken fibers. Predicted effects of time and temperature are found to agree well with experimental results for total fiber breaks, but significant disagreement in prediction of one of the model parameters occurred which suggests that the model is not a complete description of the processes involved. Mechanisms other than fiber failure which become increasingly important in cross-ply and angle-ply composites include intralaminar and interlaminar cracking. The acoustic emission curves continue to be very similar to the unidirectional specimen curves except that the lower value of n corresponds to a lower tendency to stabilize, and an increasing proportion of the emissions come from matrix damage mechanisms rather than fiber breaks.

→Originator Supplied Keywords include:

(3)

Contract A.F.O.S.R./A.R.M.I.N.E.S.

N° A.F.O.S.R.-82-0141

Final Report

August 1983

DAMAGE ESTIMATION IN CARBON FIBRE REINFORCED EPOXY AND ITS INFLUENCE ON RESIDUAL PROPERTIES

CONTRACT A.F.O.S.R./A.R.M.I.N.E.S.

N° A.F.O.S.R.-82-0141

Final Report

August 1983

DAMAGE ESTIMATION IN CARBON FIBRE REINFORCED EPOXY AND ITS INFLUENCE ON RESIDUAL PROPERTIES

A.R. BUNSELL - D. VALENTIN

INTRODUCTION AND THEORY

The use of carbon fibre reinforced plastic (c f r p) in applications for which it is necessary to be able to guarantee a minimum residual strength or lifetime is at present prevented or at least limited by our lack of understanding of failure mechanisms in this type of material. In particular time effects and the effects of repeated loading are not known. Most studies assume for example that unidirectional c f r loaded parallel to the fibres is perfectly elastic and that no creep occurs. Extensometry and mechanical tests do indicate that there is no evolution of the structure and no creep is measurable however delayed failure does sometimes occur (1) showing that the material is not truly elastic. The failure of unidirectional c f r p loaded in the fibre direction requires the failure of the fibres which can be detected using the acoustic emission technique. Fuwa, Bunsell and Harris (2) used this technique to study unnotched rectangular unidirectional specimens and showed that under cyclic loading to an unchanging maximum load the acoustic activity recorded each cycle diminished as cycling proceeded. With the exception of the first cycle all emissions were recorded just before the maximum load each cycle was reached. The acoustic emission technique indicated that the material was not behaving in a perfectly elastic manner however as cycling proceeded the material was seen to become apparently more stable. See Figure 1.

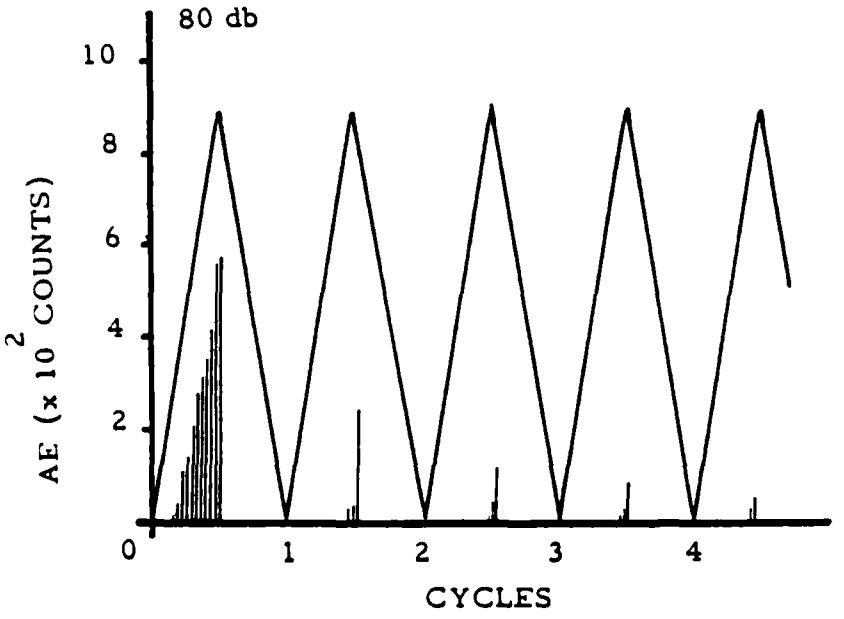

Fig. 1 : Acoustic emission recorded during cyclic loading of CFRP, after FUWA (3).

../..

The emissions recorded from these types of specimens were considered to be and indeed were shown to be related to irreversible damage occuring in the material. Exactly similar acoustic emission behaviour was observed with internally pressurised NOL rings and filament wound pressure vessels indicating that the same failure processes were occuring (3, 4). The pressure vessels which were tested were also subjected to creep tests and the acoustic activity was seen to continue after steady pressure conditions had been achieved. This emission was also seen however to decrease with time and again the structure seemed to stabilise.

The behaviour of these c f r p specimens was discussed by Fuwa, Bunsell and Harris (5) who concluded that random failure of fibres throughout the material was occuring during most of the loading. Two mechanisms were considered possible to account for the observed acoustic activity and both involved the matrix. Either the anelastic behaviour of the matrix was leading to the fibres being subjected to increased loads each cycle and so further failures were recorded or the viscoelastic properties of the matrix were leading to a redistribution of loads and this way producing further fibre breaks.

In order to study the causes for the continuing damage accumulation which had been observed in this material a close study of the creep behaviour of unidirectional c f r p was made. In this way only the mechanism involving the viscoelastic behaviour of the matrix was studied. It was found that under constant load an unidirectional c f r p specimen continues to be a source of acoustic emission which showed that mechanical degradation is still occurring. Figure 2 shows a typical curve obtained (6).

../..

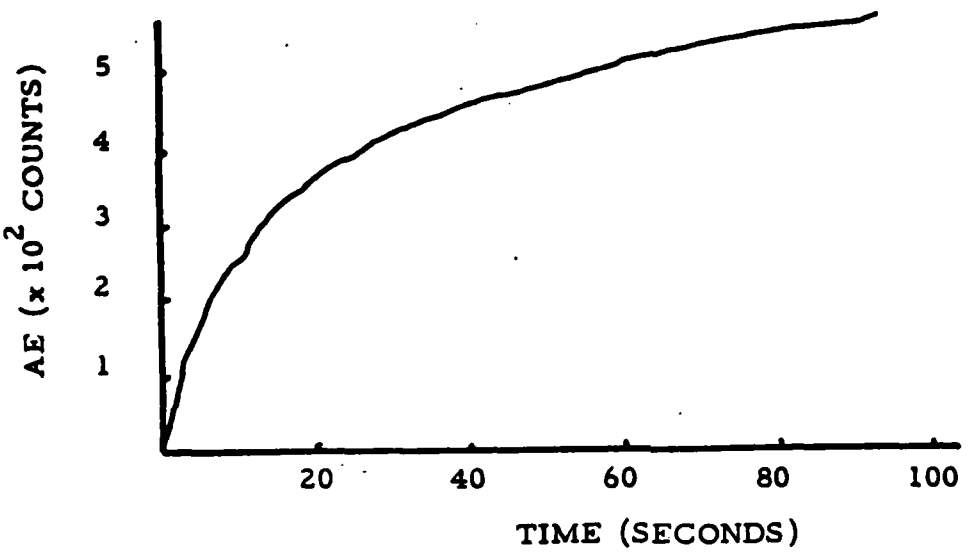

Fig.2 : Acoustic emission versus time curve obtained with an unidirectional CFRP specimen under constant load.

It was shown that the acoustic emission progressively and regularly decreased as the earlier studies had revealed, however a complete stabilisation of the material was found not to occur although the rate of emission can be extremely low. The reproducible and regular acoustic emission curves could be described by the following expression

$$N = \frac{A \ln}{} \left(\frac{t + t_o}{t_o}\right) \qquad (1)$$

where N is the total number of recorded emissions.

A is a constant for a given load but varies with the applied load level.

t is time

t_o is a time constant.

From equation (1) we obtain

$$t = t_o \exp (N/A) - t_o \qquad (2)$$

which when differentiated gives

$$\frac{dt}{dN} = to/A \quad \exp \quad (N/A)$$

so that

$$\ln \left(\frac{dt}{dN}\right) = \ln \left(t_o/A\right) + N/A \qquad (3)$$

That is to say the function ln (dt/dN) is a linear function of the total number of recorded emissions from the initial loading.

By modifying the recording equipment we were able to record directly ln (dt/dN) as a function of N which as Figure 3 shows results in an almost straight line which has a slope of 1/A.

The deviation from a perfect straight line is taken into account by adding to the emission rate equation, derived from equation 1, a factor n, where n is nearly one, so that

$$\frac{dN}{dt} = \frac{A}{(t + t_o)}^n \qquad (4)$$

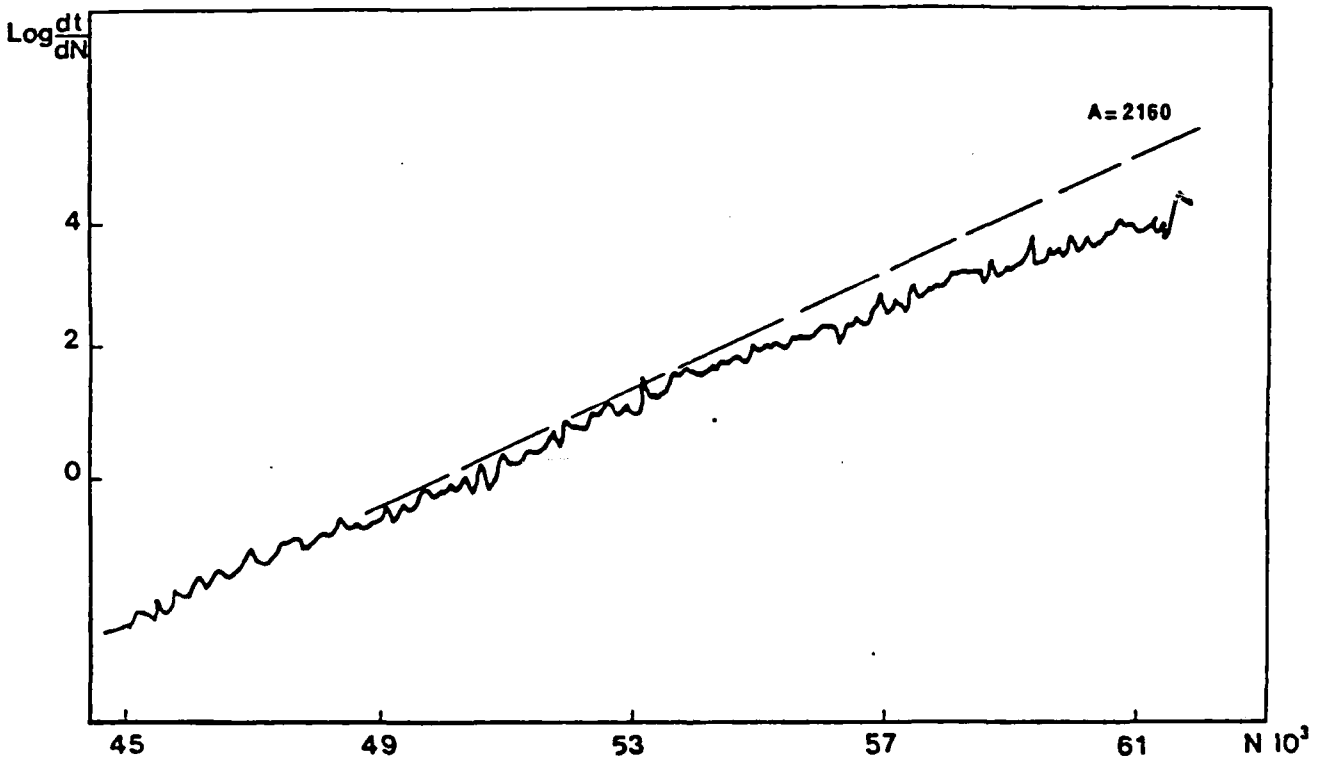

Fig. 3 : Evolution of the acoustic activity versus accumulation of emissions in a constant load test.

Any change in load level was found to have an important effect on the acoustic activity. Figure 4 shows the two possible cases an increase and a decrease in steady load level which results respectively in an increase (aa') and a decrease (bb') of activity although by very different degrees.

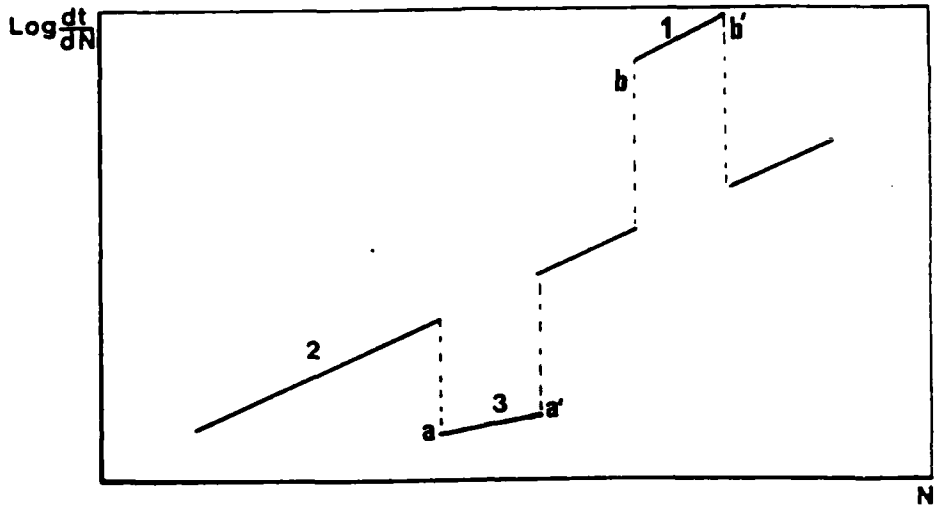

Figure 4 *Schematic representation of the effect on Ln dt/dN of varying the load level between load 1, the lowest load to load 3, the highest. Activity is seen to be a function of accumulated damage and independent of loading history.*

An overloading and then return to the original load results in additional emissions corresponding to an accelerated aging of the specimen. A reduction of load level produces greatly reduced acoustic emission activity which then increases on returning to the original load . In both cases, after a transition period of several hundred emissions a rate of emission is recorded which corresponds to an extrapolation of the original curve obtained at the same load level. The significance of this observation is that emissions recorded during overloading correspond to damage which would have occurred over a much greater length of time at the original load. A period of unloading almost arrests further damage which occurs at a very much lower rate than it would have done at the original load level. The total damage is almost independent of the load history of the specimen although the time taken to arrive at this level of damage does depend on the load history.

The experimental results have confirmed the hypothesis that with the type of specimen studied the fracture of fibres is the dominant source of acoustic emission. As the behaviour, and above all the failure of the material, are dominated by the fibres the acoustic emission which is recorded can be directly related to accumulating damage of the material.

The work of Rosen (7) and later Zweben (8) and Phoenix (9) considers a unidirectional composite as a chain of short fibre bundles with the length of each link being determined by the critical load transfer length δ . The matrix plays only a load transferring role and does not in itself contribute to the modulus or to the load bearing capability of the composite. See Figure 5.

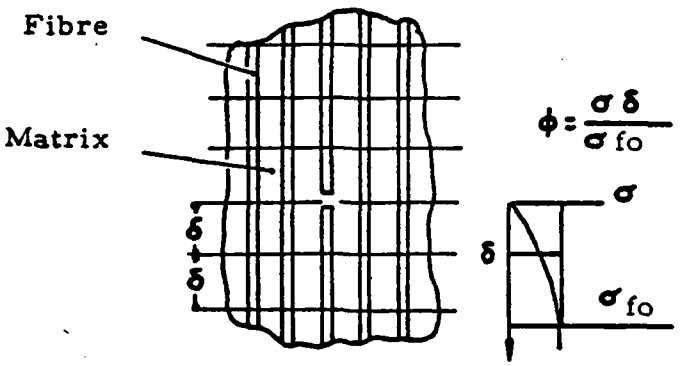

Fig. 5 : The fibre bundle chain model of a unidirectional composite material.

Taking this model we shall compare the load versus acoustic emission curve obtained for our unidirectional c f r p with the curve of the load which can be supported by a fibre bundle as a function of the number of broken fibres in that bundle, see Figure 6.

The fibres in a bundle break over a wide range of loads due to individual differences amongst the fibres and the distribution of defects on each fibre. The failure distribution as a function of applied load may be described by a Weibull distribution of the form (10).

$$\frac{N}{N_O} = 1 - \exp \left(\frac{f}{f_O}\right)^{\beta} \qquad (5)$$

where N is the number of broken fibres
N_O is the total number of fibres in the bundle
f is the load applied to each fibre
f_O is a constant
β is the shape parameter of the Weibull distribution.

The load which must be applied to each fibre to break a fraction N_o of them is therefore given by

$$f = f_o \left(\ln \frac{N_o}{N_o - N}\right)^{1/\beta} \qquad (6)$$

The load which can be supported by the bundle with N broken fibres is

$$P = (N_o - N)\ f$$

so that from equation 6 $P = (N_o - N)\ f_o \left(\ln \frac{N_o}{N_o - N}\right)^{1/\beta}$ (7)

Figure 6 represents the variation of the applied load P as a function of the fraction of broken fibres in the bundle using a value of 3 for the shape parameter β. The curve passes through a maximum which in an increasing load test is the ultimate strength of the bundle. Before reaching the breaking point however considerable numbers of fibres have inevitably been broken although where and when these breaks occur does not affect the final bundle strength. Increasing the value of β does not alterthe general form of the curve but reduces the critical fraction of fibres which needs to be broken to cause the bundle to fail.

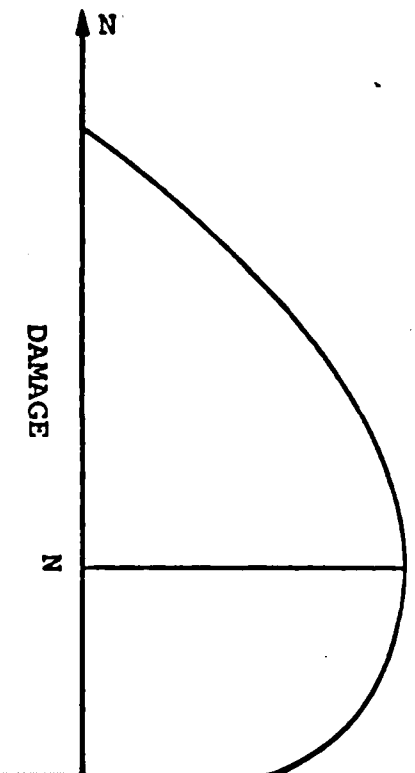

Fig. 6 : General Shape of Maximum load versus damage curve for a bundle obeying a Weibull distribution.

The load versus acoustic emission curves for unidirectional c f r p specimens are very similar up to failure to the curve of load versus fibre breaks shown in Figure 6 for a fibre bundle although in the composite case the shape parameter has a value around 5.

The behaviour shown in Figure 6 is not time dependent if the fibres are elastic so that in applying it to the c f r p specimens it is necessary to add the possibility of delayed failures occurring.

Lifshitz and Rotem (11) have proposed a model which attempts to explain the accumulation of damage in terms of the viscoelastic nature of the matrix. This time dependent behaviour is most evident in tests on cross plied material (1). In terms of the fibre bundle chain model a flowing of the matrix results in an increase in load transfer length δ, possible interaction between previously isolated fibre breaks and the effect of a break being experienced over a longer length of neighbouring fibres, so an increase in the probability of their failure.

The results of steady load tests at increasing load levels, show that the damage which occurs under steady conditions is an anticipated failure of progressively stronger fibres which would have broken at higher loads in a tensile test, Figure 7. If it is assumed that fibres break independently of their individual strengths, as in Figure 7 new fibre breaks and therefore acoustic emissions would be recorded with the smallest increase in load instead of the delay of greatly decreased activity which is observed.

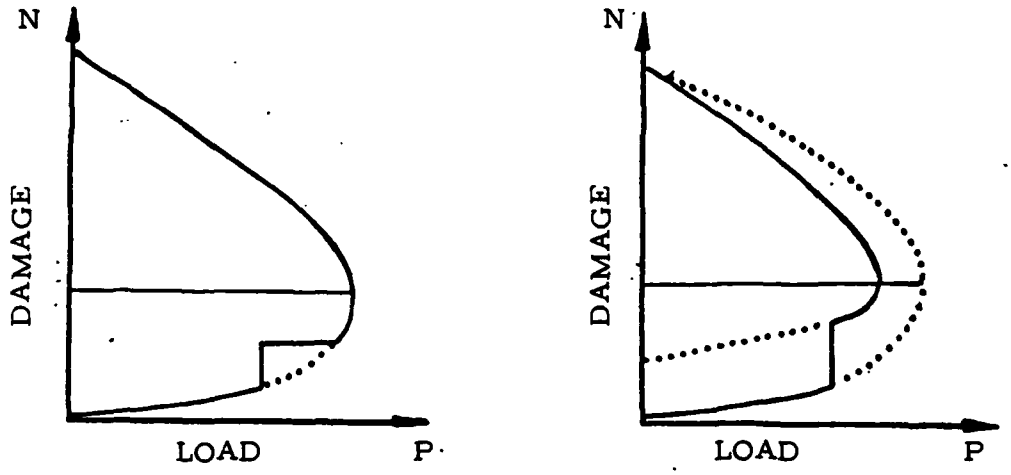

Fig. 7 : Evolution of the load bearing capability of a bundle
a) if the weakest fibres are broken first
b) if the fibres are broken randomly, without consideration for their strengths, because of stress concentrations.

Failure occurs in the composite specimen much more suddenly than for the fibre bundle and seemingly without acceleration of activity so that it is not possible to obtain all of the damage versus load curve. The fact that no acceleration of acoustic activity was detected can be understood if it is remembered that the composite specimens must be considered as a chain of fibre bundles. The acoustic emission which is recorded as coming from a unidirectional c f r p specimen originates from points all over the material as has been shown by the acoustic emission location technique using two transducers. Near failure however one of the fibre bundle links is considered to attain its ultimate tensile strength and catastrophic failure of this link occurs whilst the rest of the specimen is still in a stable state.

As there are a great number of fibre bundle links in any specimen, the length of the link being determined by the critical fibre length (< 2 mm), accelerated activity coming from one link will not make a significant change to the overall acoustic activity. In addition near to failure the damage which occurs probably ceases to be of general random nature and a concentration of breaks most likely occurs.

Minimum Life Time Prediction under Steady Loads. Whilst it is not possible to obtain all of the load versus damage curve it is clear that a specimen at its critical damage level N, corresponding to the maximum possible load, is able to support lower loads. As damage is independent of the load history the critical damage level N therefore corresponds to a guaranteed minimum failure level for all loads less than the ultimate tensile load level, Figure 8. The ultimate tensile strength can be determined by preliminary tests.

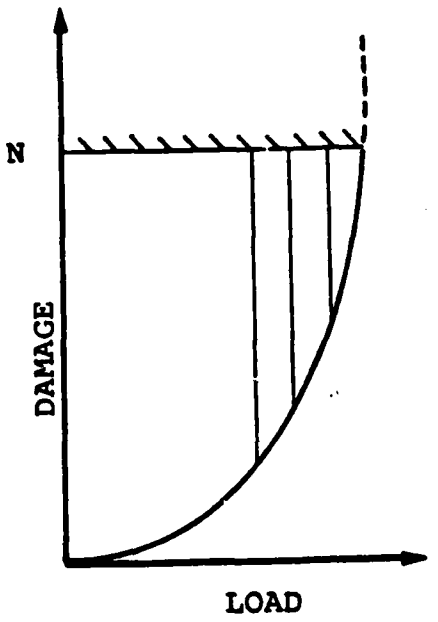

Fig 8 : Minimum value N of the damage at failure, used to compute the minimum lifetime of a material under a given load.

The type of successive steady load tests on a given specimen, as shown in Figure 5, allows the value of N to be determined approximately, although the value of N must be in arbitrary units as it is not possible to relate this directly to a precise number of fibre breaks.

It is therefore possible to calculate approximately the lifetime of the specimen under different steady load conditions as it is equal to the time required for the damage level to attain N

As the prediction of lifetime only takes into account mechanical degradation and the lifetime rapidly becomes very long as the load is reduced it should be remembered that changes in the molecular structure by aging of the matrix have not been considered in this approach.

EXPERIMENTAL DETAILS OF THE PRESENT STUDY

Rectangular flat specimens were made from CIBA GEIGY prepreg containing 914 C epoxy resin and TORAY T6K carbon fibres and were cured in an autoclave. Unidirectional and Cross plied specimens were made and the cross plied arrangements were $(0°, 90°)_s$ $(0°, 90, T)_s$, in which T represents a layer of satin weave carbon fibre cloth (±15°), (±30) and (±45°). Their thickness were 0.5 mm for the 4 layer plates and 0.8 mm for specimens containing the cloth layer. The gauge length of all specimens was 100 mm but different widtsh were used in order to assume that in all cases continuous fibres traversed the whole length of the specimen. In those specimens in which some fibres were parallel to the axis the width was 17 mm and for the (±15°), (±30°) and (±45°) specimens widths of 51 mm, 80 mm and 120 mm were used respectively. It was therefore necessary to break fibres in all cases in order to break the sample.

Unnotched rectangular specimens of pure 914 C resin have also been tested (50 x 15 x 2,5 mm) at 21°C, 60°C and 120°C.

The tensile and creep tests were conducted on appropriate tensile machine and all tests were monitored with a Dunegan Endevco acoustic emission system which comprised a D 140 B piezo electrice transducer with a resonant frequency of 200 HKz, a preamplifier with a frequency range of 100-300 KHz, and a fixed gain of 40 db and a 300 series system which served to give a total signal amplification of 80 dB. The data collection mode which was used was pulse count with a dead time between events chosen to be 100 µs. Counts were recorded on an X-Y plotter which allowed a direct trace of log dt/dN as a function of N.

../..

RESULTS AND DISCUSSION

Tensile and compression tests were conducted on the pure 914 C resin. These specimens behaved in a very brittle manner in tension and considerable scatter was observed in the tensile strength although the values of Youngs modulus were similar (4 GPa at 21°C) to that found in the literature (12). Increasing the temperature from 21°C to 120°C produced a fall in both tensile strength and modulus. Figure 9 shows that no plastic behaviour was observed in tension with the pure resin specimens. The tensile tests were limited in scope because of the extreme notch sensitivity of the resin and compression tests proved more informative. In compression and at all lovels the resin showed

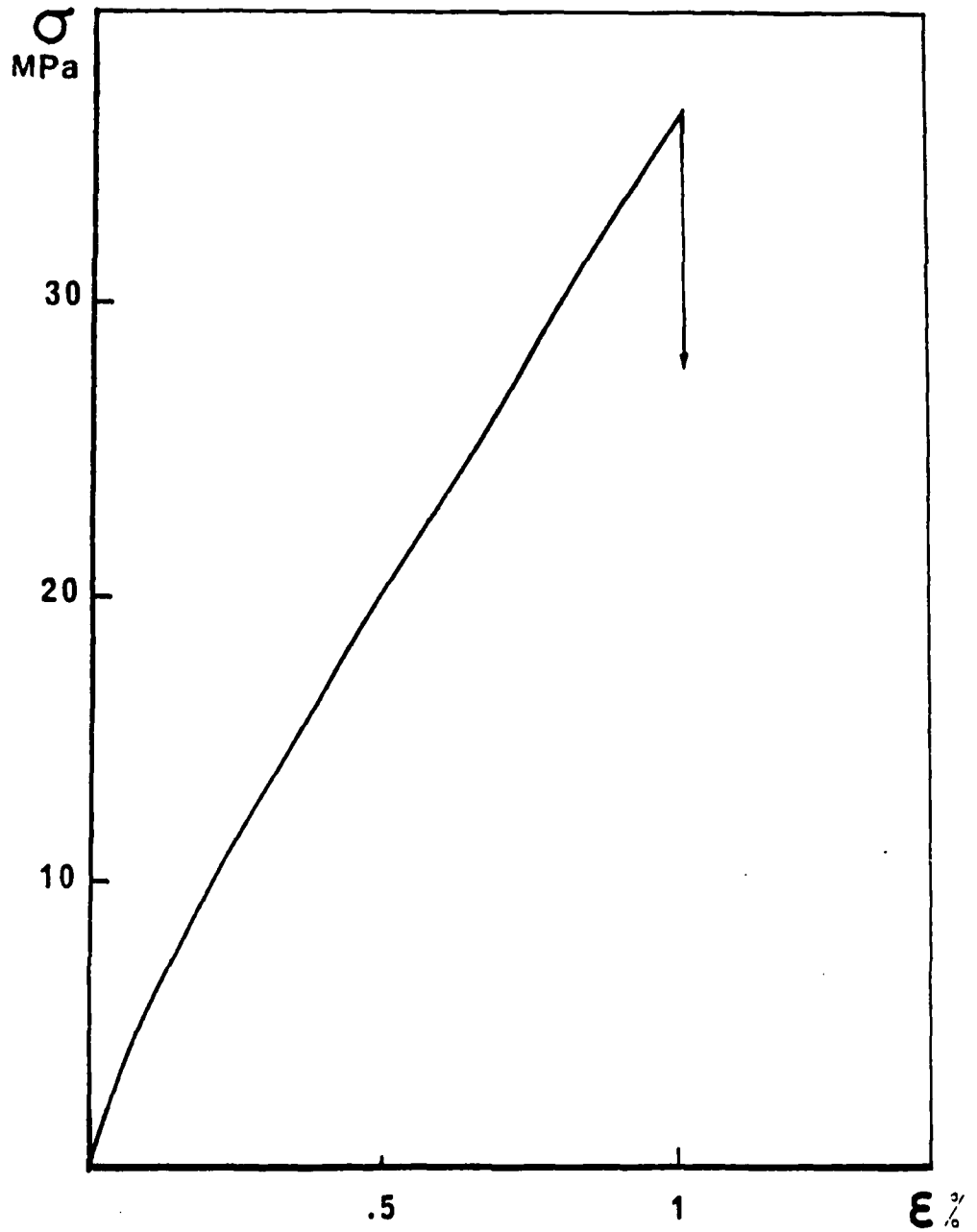

anelastic behaviour. Cyclic compressive loading revealed an hysteresis in the mechanical response of the resin and an accumulation of strain when the minimum load remained negative. The viscoelastic nature of the resin was revealed by constant load tests and as Figure 10 indicates, the creep curves were described by :

$$\varepsilon = \varepsilon_o + \alpha \text{ Log } t \qquad (8)$$

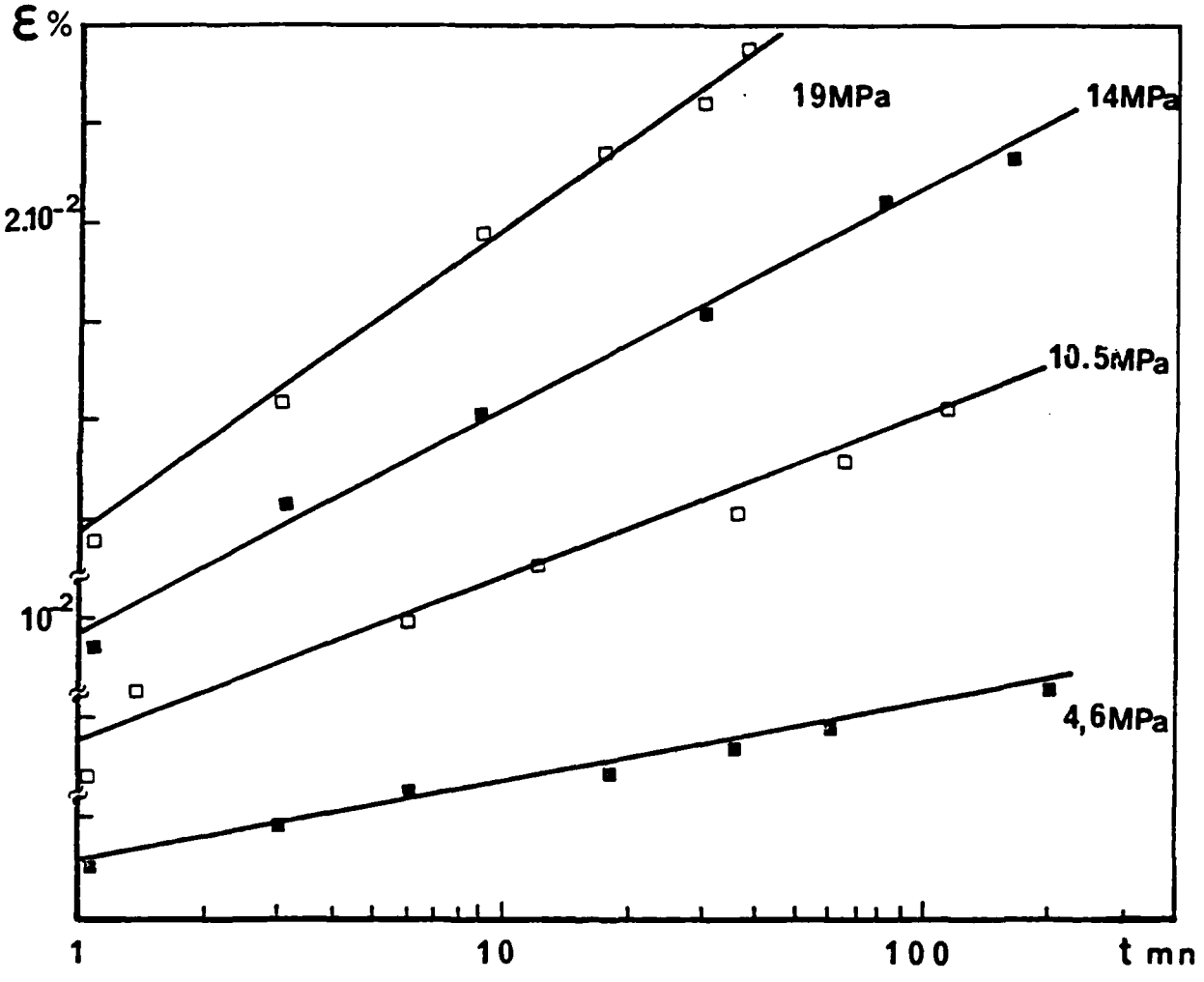

Fig. 10 : Creep curves obtained at various stress levels at room temperature.

where ε_o was the instantaneous strain produced on loading and α was a function of the applied stress such that $\alpha = K \sigma^{\beta}$. The parameters K and β were functions of the temperature as is shown by Table 1. From equation 8 it can be seen that the tensile creep modulus of the resin is given by :

$$E(t) = E_o \left(\frac{1}{1 + K E_o \sigma^{\beta-1} \text{ Log } t} \right) \qquad (9)$$

Temp. °C	K	β
20	$2.4\ 10^{-6} MPa^{-1,2}$	1,2
80	$4.98\ 10^{-6}\ MPa^{-1,32}$	1,32
120	$1.89\ 10^{-5} MPa^{-1,49}$	1,49

Table I - Variation of the K and β creep parameters as a function of temperature.

The results of steady loading of unidirectional and cross plied specimens have been reported elsewhere (13) and produced acoustic emission which was described by equation 1. Table II shows that the value of the power n in equation 4 varied with the fibre lay up. As the angles of fibre lay up increased and mechanisms other than fibre breakage became more important the value of n decreased from unity. The shape of the curve given by equation 1 depends greatly on the value of n so that it is a sensitive indicator of changes in failure mechanisms.

Specimen	0°	$(0°,90°)_s$	$(\pm 15°)_s$	(0°,90°,T°)
n	0,99	0,98	0,95	0,90

Table II - Values of n for each type of specimen

Amplitude analysis of the emission obtained from the unidirectionnal and cross plied specimens indicated that the failure of carbon fibres did not produce very energetic emissions whereas matrix cracking did (14). The curve of emission amplitudes obtained from $(0°, 90°)_s$ specimens was found to be asymmetric when the specimens were tested at different angles. This was be cause at 0° the outer-layers of the specimens contained fibres aligned parallel to the

applied load whereas at 90° those layers parallel to the loading direction were sandwiched between layers in which the fibres were aligned at right angles to the load. At 0° interlaminar shear did not play a role, tensile loading of the matrix in the central layers with fibres at 90° did exist but was suppressed by the high modulus fibres in the outerlayers. Damage was therefore predominantly by fibre failure. At 90° the outerlayer containing fibres at right angles to the load direction were less restrained and tensile failure of the matrix could occur.

FAILURE MODEL

Tensile loading : In discussing the failure of the composite plate specimens considered in this study the degradation of unidirectional specimens loaded in the fibre direction will be first considered. Later it will be shown that there arguments can be extended to cross plied specimens although the failure processes are more complex in those materials.

The failure model for unidirectional specimens has been introduced above. The original theory (7) considered that the effect of a fibre was restricted to a segment of the composite due to the shear loading of the broken ends of the fibre. In this section load from the fibre was distributed evenly on to all the remaining intact fibres in the segment. Zweben (8) considered the effect of the load being transferred primarily on to intact fibres in the neighbourhood of the break.

Recoirting equation 6 for a unidirectional composite of length L_o containing N_o fibres for which the strength probability distribution as a function of applied stress σ and fibre length L is given by :

$$F(\sigma, L) = 1 - \exp - L \left(\frac{\sigma}{\sigma_o}\right)^{\beta} \qquad (10)$$

../..

The length of fibre in the composite which should be taken δ must be related to the critical load transfer length. In this case the composite can be considered to consists of N_o separate chains having L_o/δ links. In such an arrangement the number of breaks recorded for a given applied stress on the fibre σ_f without taking into account any redistribution of stress due to broken fibres will be :

$$N_1 = N_o \frac{L_o}{\delta} F(\sigma, \delta) \qquad (11)$$

Rosen (7) gave the following expression for δ

$$\delta = \frac{1}{2} d \left[\frac{E_f}{G_m} \frac{1 - V_f^{1/2}}{V_f^{1/2}}\right]^{1/2} \text{Cosh}^{-1} \left[\frac{1 + (1 - \phi)^2}{2(1 - \phi)}\right] \qquad (12)$$

where d is the fibre diameter and ϕ is defined for the relation $\sigma(\delta) = \phi\,\sigma$, $\sigma(\delta)$ is the stress in the fibre at the distance δ from the break and σ the stress in the unbroken fibre.

In the case where no stress concentration occurs the stress supported by the intact fibres is given by :

$$\sigma_f^* = \frac{\sigma_f}{1 - F(\delta, \sigma_f)} \qquad (13)$$

where

$$\sigma_f = \frac{\sigma_c}{V_f} \left[1 - \frac{E_m}{E_d}(1 - V_f)\right]$$

and the total number of broken fibres will be

$$N_T = N_o \frac{L_o}{\delta} F(\sigma_f^*, \delta) \qquad (14)$$

../..

In the case where only neighbouring fibres take up the dumped load a concentration factor K must be determined, so that they support $K\,\sigma_f$.

If an hexagonal fibre arrangement is considered the probability of i-1 fibres neighbouring a broken fibre would break is given by :

$$P\ i/_1 = C_6^{i-1} [F\ (K_1\ \sigma_f) - F\ (\sigma_f)]^{i-1} \quad x$$

$$[1 - F\ (K_1\ \sigma_f) + F\ (\sigma_f)]^{7-i} \qquad (15)$$

The number of fibres broken by stress concentration due to one broken fibre is :

$$N_2 = N_2 \times P_{2/1} \qquad (16)$$

N_2 represents the number of double neighbouring breaks.

In the case of two neighbouring fibres being broken the number of fibres which will break is given by :

$$N_3 = N_1\ [P_{3/1} + P_{2/1} \times P_{3/2}] \qquad (17)$$

where $P_{3/2}$ represents the probability of breaking two fibres in cascade from one original break.

$$P_{3/2} = 5\ [F\ (K_2\sigma) - F\ (K_1\sigma)]\ \gamma + 3\ [F\ (K_2\sigma) - F\ (\sigma)]\ \beta \qquad (18)$$

with $\gamma = [1 - F\ (K_2\sigma) + F\ (\sigma)]^4\ [1 - F\ (K_2\sigma) + F\ (K_1\sigma)]^3$

$\beta = [1 - F\ (K_2\sigma) + F\ (\sigma)]^3\ [1 - F\ (K_2\sigma) + F\ (K_1\sigma)]^4$

The total number broken fibres will be given by :

$$N_r = N_1 + N_2 + N_3 \qquad (19)$$

Table III shows the number of fibre breaks calculated to occur in a unidirectional specimen such as has been tested in this study consisting of 100 000 fibres. At room temperature δ was calculated to be 55 µm, with G_M = 1500 MPa and a Poissons ratio of 1.4. The diameter of the fibres was 7 µm and E_f was 240 GPa. The value of K_1 was obtained by taking the case in which the load supported by one fibre prior to break was distributed between its six neighbours and for K_2 when the load supported by a pair of fibres was distributed between their eight surrounding neighbours. In this way it is possible

MPa	K_1 = 1,16 K_2 = 1,25		
	N_T	N_2	N_3
153	7		
307	122		
461	621		
615	1964		
769	4795		
923	9945	2	
1077	18429	9	
1231	31449	26	
1384	50398	67	
1538	76864	155	0,61

Table III

Number of fibre breaks calculated to occur in a unidirectional specimen during a tensile test.

to compare the experimantal results with those calculated with different Weibull parameters σ and β . It can be seen in Figure 11 that a value for σ_o of 1.5 GPa M^{-4} for a Weibull shape parameter β of 4 gives a good correlation and are similar to those values found in the literature (15). The effect of the stress concentration on the number of emissions is small as only a few hundred emissions are attributable to the coefficient K_1. It has been suggested (7) that defect size which is to say the number of adjacent breaks is the controling

../..

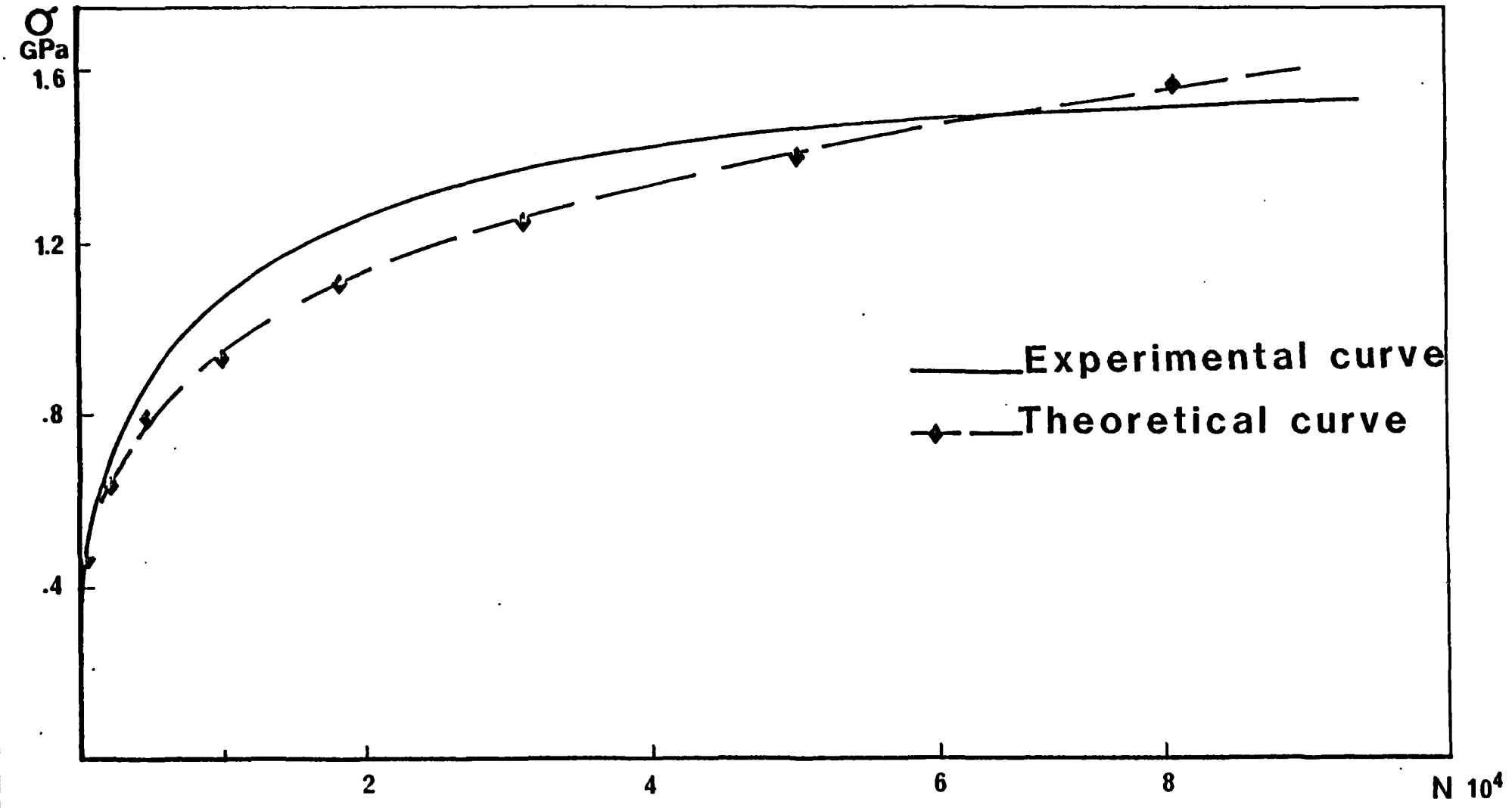

Fig. 11 : Comparison between experimental and simulated tensile test curves.

parameter in composite failure. Dissolution of the matrix has revealed, in this study, cases of three adjacent breaks. Some authors (16-18) suggest that the Weibull shape parameter for the fibres (β_f) can be related to the shape parameter of the composite through :

$$\beta_c = i \ \beta_f \tag{20}$$

where i is the number of adjacent breaks. In this study β_f was found to be 4 and β_c 12 so that the premise that three adjacent breaks provoked the final failure was supported.

TIME EFFECTS

In considering the effect of prolonged loading stress concentration shall be ignored as relaxation of the matrix reduces their importance. It is the effect of time on the load transfer length which is considered important. The gradual increase in load transfer length will have the effect of increasing the stresses in intact fibres in adjacent segments so that the number of load supporting fibres in these segments can be written as :

$$R\ (t = 1) = F\ (\dot{\sigma_f}^*\ (t = o))\ [\frac{\delta\ (1)}{\delta\ (0)} - 1] \tag{21}$$

where $F\ (\sigma_{fe} = t = O)$ is the initial number of broken fibres at the beginning of the creep test. The stress on the fibres will increase so that :

$$\sigma_f^*\ (t - 1) = \frac{\sigma_f}{[1 - F\ (\sigma_f)][1 - R\ (t = 1)]} \tag{22}$$

and will provoke further fibre breaks so that the total number of emissions will be :

$$N_r = N_o \frac{L_o}{\delta(o)} F\ (\sigma_f^*\ (t = 1),\ \delta\ (o)) \tag{23}$$

../..

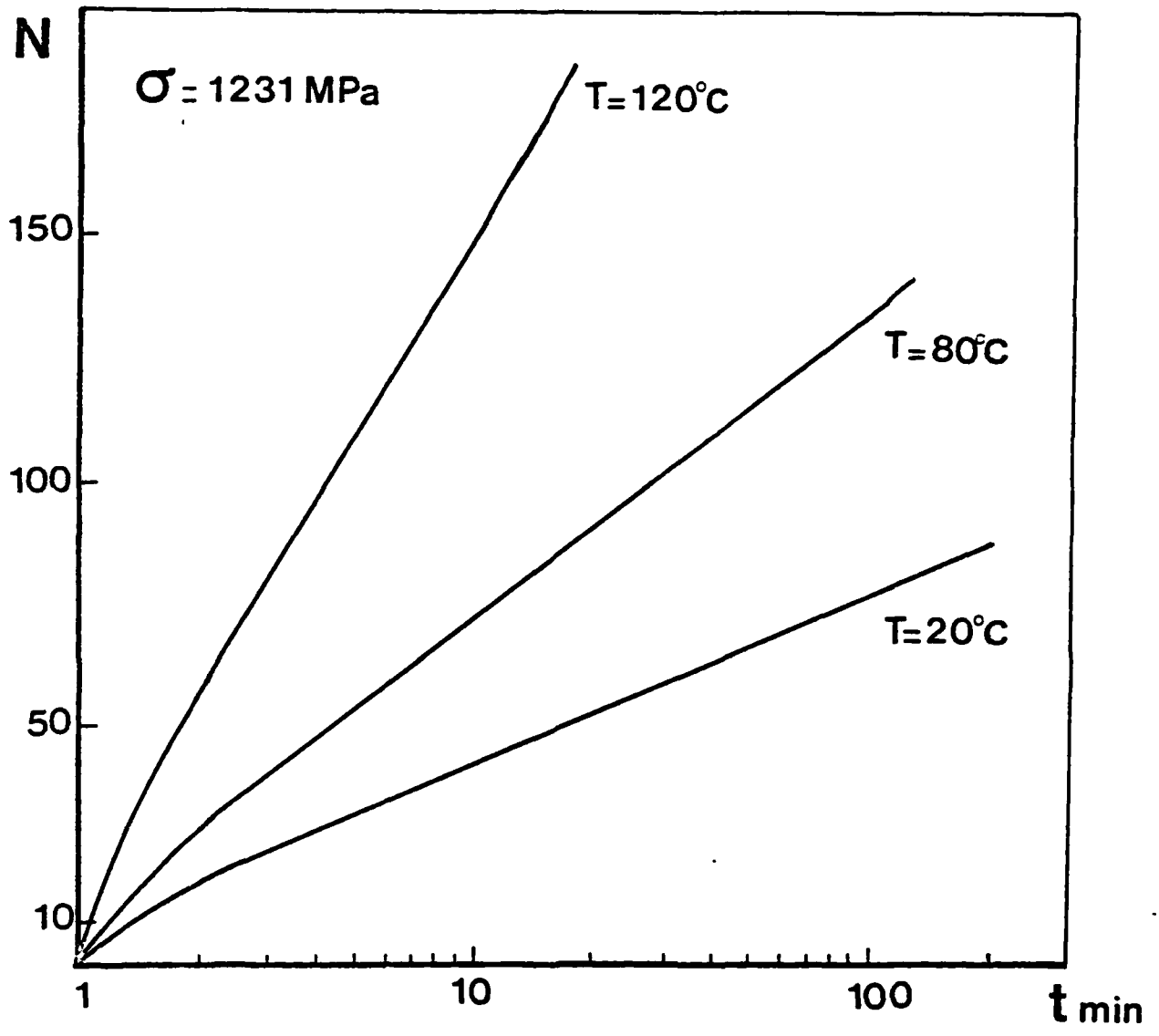

Fig. 12 : Simulated curves for steady loading conditions at 20°C, 80°C and 120°C. The values of δ temp. were :

$$\delta_{20} = 55\ 10^{-6}\ |1 + 10^{-2}\ \sigma^{0,2}\ \text{Log}\ t\ |^{0,5}$$

$$\delta_{80} = 57\ 10^{-6}\ |1 + 1,93\ 10^{-2}\ \sigma^{0,32}\ \text{Log}\ t|^{0,5}$$

$$\delta_{120} = 70\ 10^{-6}\ |1 + 4,9\ 10^{-2}\sigma^{\ 0,49}\ \text{Log}\ t\ |^{0,5}$$

As the load transfer length aroung the original and later breaks will continue to increase, the number of fibres unavailable to support the load as time t is given by :

$$R(t) = F\ (\sigma_f^*\ (t=o)\ (\frac{\delta(t)}{\delta(o)} - 1)$$

$$+ \sum_{j=1}^{n=1} (\delta\ \frac{(t_n - j)}{\delta\ (o)} - 1[F\ (\sigma_f^*\ (t_i)) - F\ (\sigma_f^*(t_j - _i))] \qquad (24)$$

and

$$\sigma_f^*\ (t) = \frac{\sigma_f^*(t-1)}{1 - F\ (\sigma_f)} \times \frac{1}{1 - R\ (t)} \qquad (25)$$

so that the combined number of broken fibres due to tensile loading and creep will be :

$$N_T\ (t) = N_o\ \frac{L_o}{\delta(o)}\ F\ (\sigma_f^*\ (t),\ \delta(o)) \qquad (26)$$

A simulated steady load test using equation 26 predicts a logarithmic accumulation of damage as shown by Figure 12 and is therefore similar to the experimental behaviours. The variations predicted for A given in equation 12 are of the form $A = \lambda\ e^{k\sigma}$ which corresponds to experimental observation where λ and k are constants. This approach gives a value for k of 4×10^{-3} MPa^{-1} which compares well with the experimental value of $4.6. \times 10^{-3}$ MPa^{-1}. The predicted effects of temperature on the variation of the values of A were found to agree with the experimental results. Table IV shows that the calculated ratios of A_{80}/A_{20} and A_{120}/A_{80} corresponded well to the experimental values of 2.7 to 2.8 and 2.4 to 2.7 respectively. However the calculated value of λ (0.1) is only one percent of the experimental value. This observation together with the necessity for the load transfer length to increase as a function of time more than is reasonable, suggests that the model is not a complete description of the processes which are involved however it does go a considerable way towards explaining the observed acoustic emission behaviour.

../..

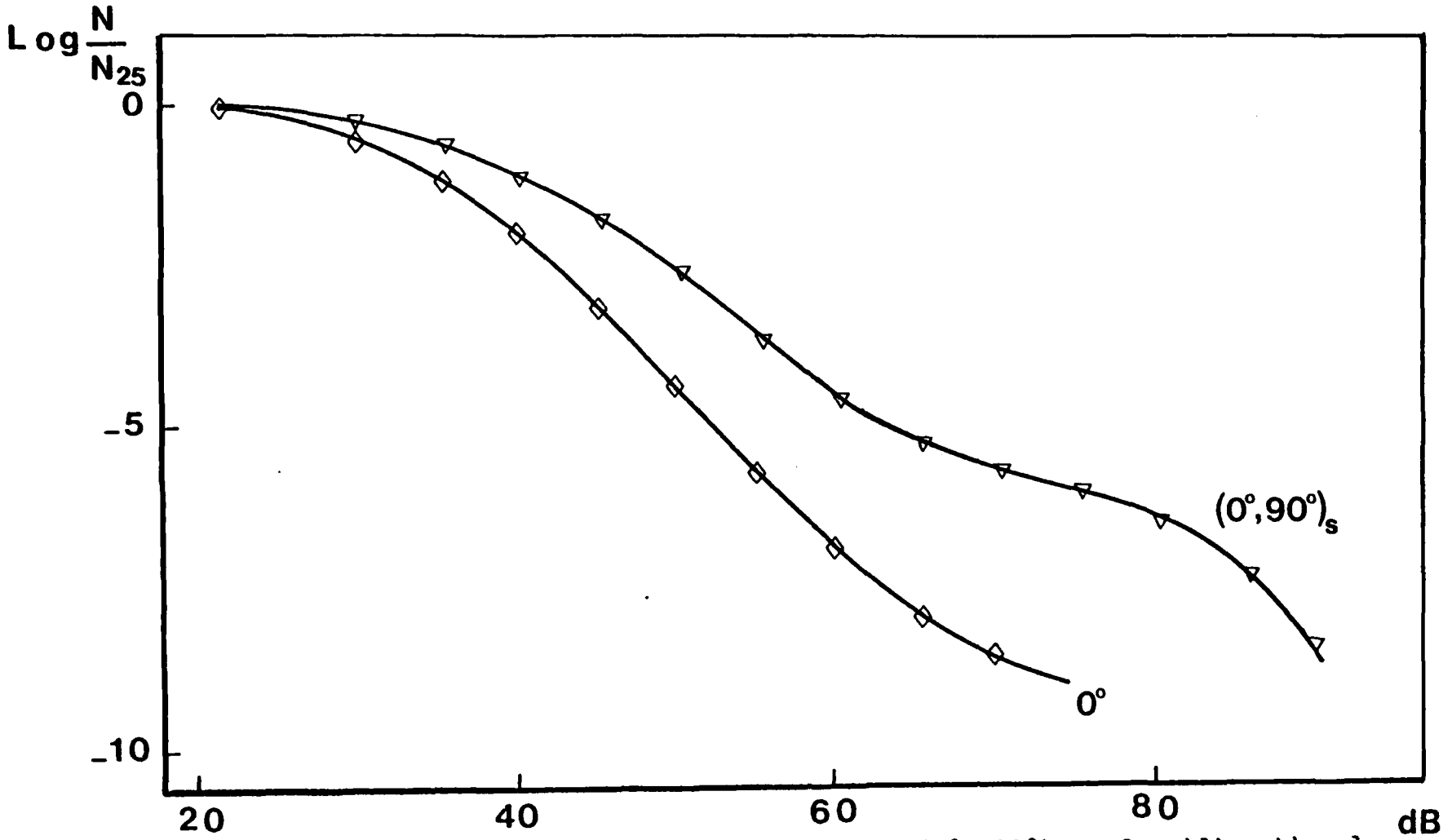

Fig. 13 : Histograms of emission amplitude of $(0°, 90°)_s$ and unidirectional specimens during tensile test.

MPa	A_{20}	A_{80}	A_{120}	$\frac{A80}{A20}$	$\frac{A120}{A80}$
769	2,17	3,47	8,26	1,6	2,38
923	4,63	8,26	18,2	1,72	2,21
1077	9,56	16,5	35,6	1,72	2,16
1231	18	30,8	64,7	1,71	2,1
1384	33,5	54	111	1,61	2,06
1538	58	91,3	183	1,57	2

Calculated values of A_{20}, A_{80} and A_{120}. The ratios A_{80}/A_{20} and A_{120}/A_{80} correspond well to the experimentally determined values of 2.7 to 2.8 and 2.4 to 2.7 respectively.

Table IV

Additional Processes : It has been observed that the parameter n used in equation 4 is a sensitive indicator of damage processes and as mechanisms other than fibre failure become increasingly important its value decreases from unity. These other mechanisms in the specimens which have been tested in this study have been observed to be intra-and inter-lamina cracking. The number of emissions recorded with the (0°, 90°) and (0°, 90°, T) specimens during tensile loading was found to be similar to that recorded with the unidirectional specimens. Figure 13 shows that there is little difference between the amplitude distributions obtained with unidirectional and (0°, 90°) specimens. It has been calculated that only 12 % of the emissions recorded from the (0°, 90°) composite came from cracking of the transverse layers which explains the similarity in tension. Under creep conditions the amplitude distributions of both types of specimens are very similar which suggests that matrix cracking is not initiated under the steady load conditions. The existences of the matrix cracks generated when the load was applied could be expected to lead to increased stress redistribution during steady loading and a higher incidence of delayed fibre failure. This is reflected in a lower value of n which describes a lower tendency of the composite to stabilize.

In the case of the (±15°) and (±30°) composites the redistribution of the intra-and interlaminar shear forces must control the accumulation of damage under steady loading conditions. The acoustic emission curves obtained from these specimens are very similar to those obtained from unidirectional specimens except that a lower value of n is observed corresponding to a lower tendency to stabilize. In the case of the (45°) specimens the interlaminar shear forces can lead to interlaminar cracking and a complete change in the origins of the emissions as has been discussed elsewhere (6).

CONCLUSION

The accumulation of acoustic emission from many carbon fibre reinforced epoxy resin plate specimens subjected to prolonged steady loading is reproducible and quantifiable. A model has been proposed based on the accumulation of irreversible damage of the composite during steady loading which goes part of the way towards explaining the observed behaviour.

REFERENCES

1. J.B. STURGEON, R.I. BUTT and L.W. LARKE.
"Creep of carbon fibre reinforced plastics"
RAE Technical Report 76168 (1976).

2. M. FUWA, A.R. BUNSELL and B. HARRIS.
"Tensile failure mechanisms in carbon fibre reinforced plastics".
J. Mat. Sci. 10 (1975), 2062.

3. M. FUWA, B. HARRIS and A.R. BUNSELL.
"Acoustic emission during cyclic loading of carbon fibre reinforced plastics".
J. Phy. D 8 (1975), 1460.

4. A.R. BUNSELL.
"Acoustic Emission for proof testing of carbon fibre reinforced plastics".
NDT Int. (1977), 21.

5. M. FUWA, A.R. BUNSELL and B. HARRIS.
"Acoustic emission studies of filament wound carbon fibre reinforced rings and pressure ressels.
J. Strain Analysis Vol. 11, N° 2 (1976), 97.

6. D. LAROCHE and A.R. BUNSELL.
"Stress and time dependent damage in carbon fibre reinforced plastics".
Advances in Composites Materials, Vol. 2 (1980), 985 Ed.
A.R. BUNSELL et Al. Pub. Pergamon.

7. B.W. ROSEN
"Tensile failure of fibrous composites". AIAA Journal 2 (1964), 198

8. C. ZWEBEN
"A bounding approach to the strength of composite materials".
Eng. Fract. Mech. Vol. 4 (1972), 1.

9. S.L. PHOENIX
"Statistical aspects of failure of fibrous materials".
ASTM STP 674 (1979, 455 Ed. S.W. TSAI.

10. W. WEIBULL
"A statistical distribution function of wide applicability".
J. App. Mech. 18 (1951), 293.

11. J.M. LIFSHITZ and A. ROTEM.
"Time dependent longitudinal strength of unidirectiona' fibrous composites".
Fibre Sci. & Tech. 3 (1970), 1.

12. D.B.S. BERRY, B.I. BUCK, A. CORNWELL and L.N. PHILLIPS.
"Handbook of resin properties".
Published by Yarsley Testing Laboratories. Oct. 1975.

13. A.R. BUNSELL, D. LAROCHE and D. VALENTIN.
"Damage and failure in carbon fibre reinforced epoxy resin".
ASTM-STP Long term behavior of composites. To be published.

14. D. VALENTIN, Ph. BONNIAU and A.R. BUNSELL.
"Failure mechanisms discrimination in carbon fibre reinforced epoxy".
To be published in Composites.

15. J.W. HITCHON and D.C. PHILLIPS.
"The dependance of the strength of carbon fibres on length".
Fibre Sci. and Tech. (12) (1979), 217.

16. S.B. BATDORF.
"Tensile strength of unidirectionaly reinforced composites".
Part 1 - J. Reinforced Plastics and Composites. Vol. 1 (1982), 15

../..

17. S.B. BATDORD.
"Tensile strength of unidirectionaly reinforced composite".
Part II - J. Reinforced Plastics and Composites. Vol. 1 (1982), 153.

18. P.W. MANDERS, M.G.BADER and T.W. CHOU - Monte Carlo.
"Simulation of the strength of composite fibre bundles".
Fibre Sci. and Tech. 17 (1982), 183.

END

FILMED

4-85

DTIC